STARVATION EFFECTS IN ELASTO-HYDRODYNAMICALLY LUBRICATED LINE CONTACTS

Rajesh Kumar[1] , Punit Kumar[2], Munish Gupta[3]

[1,3]Department of Mechanical Engineering,
Guru Jambheswar University of Science & Technology, Hisar, Haryana, India
Email id : rajesh9355@gmail.com , mcheeka@rediffmail.com

[2]Department of Mechanical Engineering,
National Institute of Technology, Kurukshetra, Haryana, India
E-mail id : punkum2002@yahoo.co.in)

Abstract

A lubricated contact suffers from starvation when the lubricant does not fill the contact inlet adequately. Such a situation arises due to short lubricant supply or at extremely high speeds. The starvation effect is modeled by shifting the position of the inlet meniscus towards the contact zone. The degree of starvation, so obtained, is plotted as a function of the position of inlet meniscus under different operating conditions. Various degrees of starvation are obtained by shifting the inlet meniscus from its fully flooded position toward the Hertzian contact zone. In this work, the effect of starvation on the two most important parameters necessary for EHL performance evaluation which are coefficient of friction and central film thickness has been studied at different loads and rolling speeds.

Key word: *Elastohydrodynamic lubrication, Film thickness, Coefficient of friction, Starvation, line contacts.*

1. Introduction

Elastohydrodynamic lubrication (EHL) is a form of hydrodynamic lubrication in which the elastic deformation of mating surfaces and piezo-viscous increase in lubricant viscosity assists largely in the formation of a load carrying fluid film. EHL is a typical mode of lubrication in highly concentrated line and point contacts involved in mechanical components such as gears, cams and roller bearings.

The prediction of film thickness and traction coefficient under realistic conditions has been the focus of attention for last five decades. The relevant literature includes several studies on thermal and non-Newtonian effects [1-7] on EHL characteristics. However, a commonly encountered practical problem attributed to inadequate filling of inlet conjunction – generally referred to as "starvation"- has not received due consideration. Due to inadequate filling of the conjunction, the EHL film generated is much thinner as compared to the corresponding

fully- flooded film and as a consequence, traction coefficient is also very high. Starvation is found to occur due to high speeds, highly viscous lubricants and limited lubricant supply [9]. Since most of the theoretical studies [9, 10] on starvation deal with its effect on lubricant film thickness only, the present study focuses on the effect of starvation on traction coefficient in addition to film thickness using full EHL line contact simulations with Newtonian fluid model.

2. Governing Equations

2.1   Reynolds Equation

The equation which governs the generation of pressure in lubrication films is known as Reynolds equation and it forms the foundation of hydrodynamic lubrication analysis. The classical Reynolds equation is given below in dimensionless form

$$\frac{\partial}{\partial X}\left(\frac{\overline{\rho}H^3 \partial P / \partial X}{\overline{\eta}}\right) - K\frac{\partial}{\partial X}\left(\overline{\rho}H\right) = 0 \tag{1}$$

Where, $K = \dfrac{3U\pi^2}{4W^2}$

Boundary Conditions
Inlet boundary condition
$$P = 0 \; at \; X = X_{in} \tag{2}$$
Outlet Boundary Condition
$$P = \frac{\partial P}{\partial X} = 0 \; at \; X = X_0 \tag{3}$$

2.2   Film Thickness Equation

The film thickness, h, at any point in an EHL conjunction is

$$h = h_0 + \frac{x^2}{2R} + v \tag{4}$$

Where h_0 is the offset film thickness, v contributes to the surface normal displacement and the method adopted for its calculation is discussed subsequently.
The film thickness in non-dimensional form is given by

$$H(X) = H_0 + \frac{X^2}{2} + \overline{v} \tag{5}$$

Where $\overline{v} = vR/b^2$ is the non-dimensional surface displacement .

2.3   Density-Pressure Relationship

The present analysis uses Dowson and Higginson density-pressure relationship:

$$\bar{\rho} = \left(1 + \frac{0.6 \times 10^{-9} P.p_h}{1 + 1.7 \times 10^{-9} P.p_h} \right) \tag{6}$$

2.5   Viscosity-Pressure Relationship

The Roelands' viscosity-pressure relationship is used in the present analysis:

$$\bar{\eta} = \exp\left[(In\eta_0 + 9.67)\left\{ -1 + \left(1 + 5.1 \times 10^{-9} P.p_h \right) \right\} \right] \tag{7}$$

2.6   Load Equilibrium Equation

The pressure developed in the lubricant supports the applied load. Therefore, the pressure distribution obtained from the Reynolds equation should satisfy the following condition.

$$\int_{x_i}^{x_a} p\,dx = w \tag{8}$$

where w is the applied load per unit width.

3.   Solution Procedure

The steps involved in the overall solution scheme are given below:
The pressure distribution[P], offset film thickness H_o and outlet boundary co-ordinate X_o are initialized to some reference values.

The current pressure distribution is used to calculate surface displacements $\left[\bar{v} \right]$ using equation (3.12).

$$\bar{v}_i = \sum_{j=1}^{N} D_{ij} P_j \tag{9}$$

where

$$D_{ij} = \frac{1}{\pi} \left[\left(i - j + \frac{1}{2} \right)\Delta X \left\{ In\left(\left| i - j + \frac{1}{2} \right| \Delta X \right) - 1 \right\} \right.$$

$$\left. - \left(i - j - \frac{1}{2} \right)\Delta X \left\{ In\left(\left| i - j - \frac{1}{2} \right| \Delta X \right) - 1 \right\} \right]$$

The surface displacements $[\bar{v}]$ are used along with the offset film thickness H_o to evaluate the fluid film thickness, H, at every node. The fluid density and viscosity are updated as per the current values of pressure. The Reynolds equation is discretized using mixed second order central and first order backward differencing scheme. It is then solved along with the load balance equation using Newton-Raphson technique to obtain an improved pressure distribution. The steps 2-5 are reiterated till a relative accuracy of 10^{-4} is achieved.

4.   Results And Discussion

4.1 Effect of Load

Fig. 1 compares the variation of the degree of starvation (σ) with the position of inlet meniscus (X_{in}) for three different values of maximum Hertz pressure (p_H=0.5, 1 and 2GPa) while the rolling velocity is kept constant at u_o=0.1 m/s. The degree of starvation (σ) is defined as the fractional loss in the weighted mass flow rate:

$$\sigma = 1 - \frac{\left\{\rho h_c u_o \left[KH - \frac{H^3}{\bar{\eta}} \frac{\partial P}{\partial X} \right]\right\}_{Starved}}{\left\{\rho h_c u_o \left[KH - \frac{H^3}{\bar{\eta}} \frac{\partial P}{\partial X} \right]\right\}_{Fully-flooded}} \qquad (10)$$

As apparent from Fig. 1 X_{in} = -6 corresponds to σ = 0 and hence, fully flooded condition, whereas, X_{in} = -1 marks the beginning of the contact zone. It can be seen from Fig. 1 that σ increases gradually with an initial shift in the inlet meniscus towards the contact zone. As the inlet meniscus approaches closer to X_{in} = -1, an abrupt increase in the degree of starvation is observed. However, this steep increase in the degree of starvation is noticed much later at p_H=2 GPa than at p_H =0.5 GPa. This is consistent with the well-known fact that the pressure distribution in an EHL contact approaches the Hertzian distribution at high loads, which implies that the pressure build-up starts quite close to the beginning of contact zone and hence, the inlet zone shrinks significantly. This observation is useful while selecting the inlet boundary for fully flooded condition at a given load.

Fig. 2 compares the pressure distributions and film profiles for two different positions of the inlet meniscus (X_{in} = -6 and -1.05) at p_H=0.5GPa and u_o=0.1 m/s. It can be seen that even though an appreciable amount of pressure is generated within the inlet for X_{in}=-6, the contact zone pressures differ only marginally for the two positions of inlet meniscus considered here. However, the film profiles clearly show the effect of starvation as the film at X_{in}=-1.05 is much thinner than that at X_{in}= -6. This film-thinning is the most serious consequence of inadequate filing of the EHL conjunction as it may lead to film failure leading to metal-metal contact and hence, increased friction and wear. Further, in order to study the effect of load, Fig. 3 shows the same characteristics as in Fig. 2 at a much higher load, i.e., p_H=2GPa keeping the other parameters same. It is quite apparent that pressure within the inlet zone reaches a negligibly small value unlike the case of p_H=0.5 GPa (Fig. 2). Also, the film profiles at the two inlet meniscus positions indicate a much less pronounced starvation effect.

As mentioned above, starvation causes an increase in the value of coefficient of friction (COF). This effect may be quantified in terms of the ratio of COF values obtained under starved and fully flooded conditions. The variation of this ratio with the degree of starvation is compared at p_H=1 and 2 GPa with u_o fixed at 0.1 m/s. It can be seen that coefficient of friction increases by factors exceeding 2, which is quite high. Also, it is apparent that at higher load, the maximum increase in COF is higher. The reason for this increase in coefficient of friction due to starvation can be understood by considering the factors on which it depends, i.e., contact zone viscosity and shear rate. The contact zone viscosity remains almost unaffected as it is observed that pressure does not undergo any noticeable change. The shear rate, however, increases due to the film-thinning caused by starvation. This increase in the shear rate results in higher shear stresses and hence, higher coefficient of friction.

Fig. 5 shows the variation of central film thickness with the degree of starvation at p_H= 0.5, 1 and 2 GPa. The slope of the curve increases with decreasing load. Under fully flooded condition, $\sigma = 0$, the difference between the central film thickness values at the three loads is maximum. This gap decreases with increasing degree of starvation and the central film thickness tends to converge to a common value independent of the load.
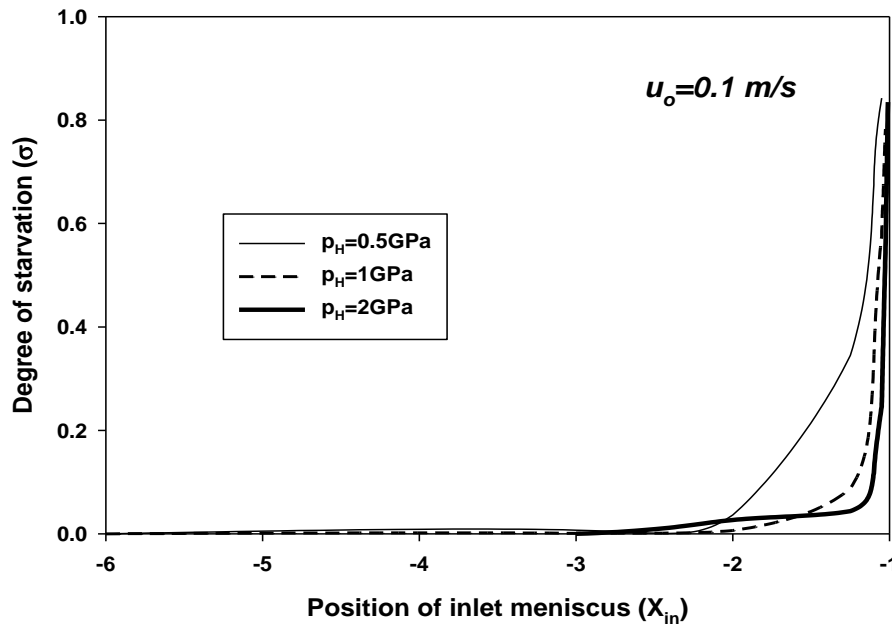

Fig. 1 : Variation of the degree of starvation with the position of the inlet meniscus for different Hertzian pressures at u_o=0.1 m/s, α=20 GPa^{-1} and R=0.02 m
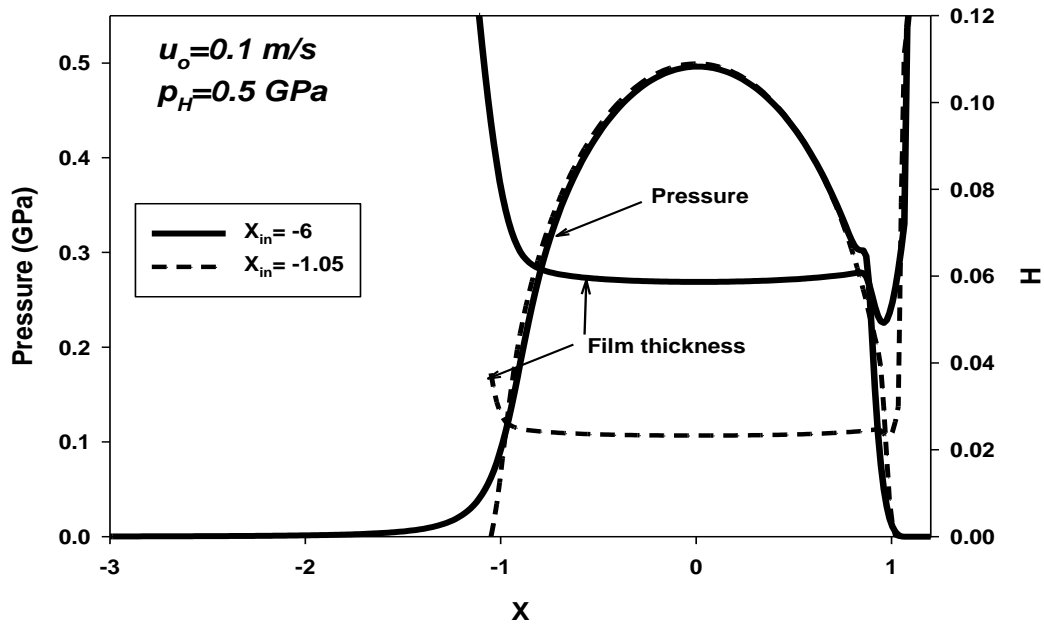
Fig. 2 : Comparison of pressure distributions and film shapes at two different positions of inlet meniscus for p_H=0.5 GPa, u_o=0.1 m/s, α=20 GPa^{-1} and R=0.02 m
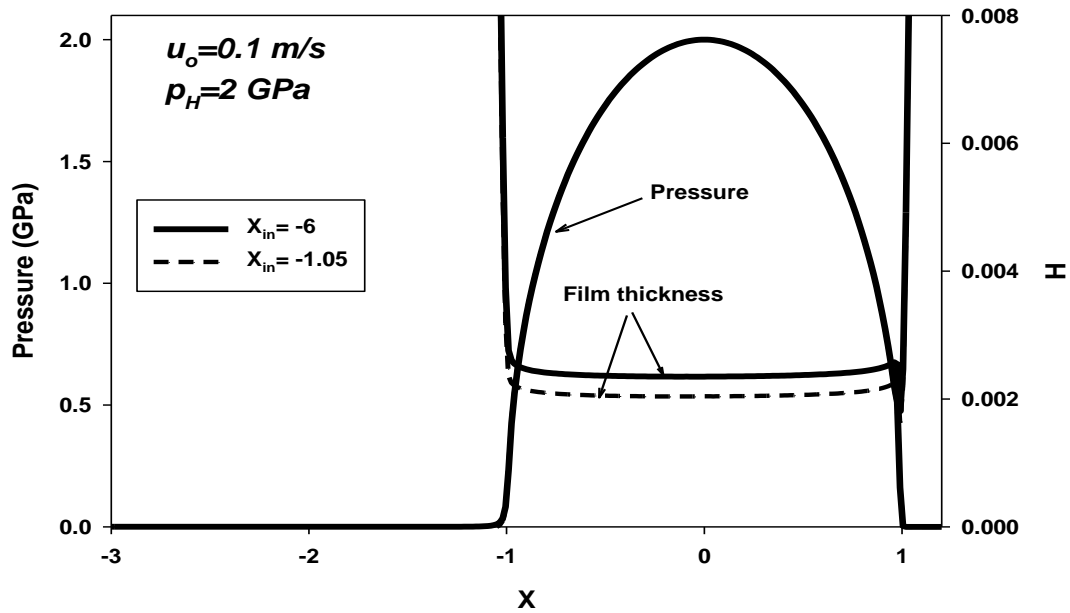

Fig. 3: Comparison of pressure distributions and film shapes at two different positions of inlet meniscus for p_H=2 GPa, u_o=0.1 m/s, α=20 GPa^{-1} and R=0.02 m
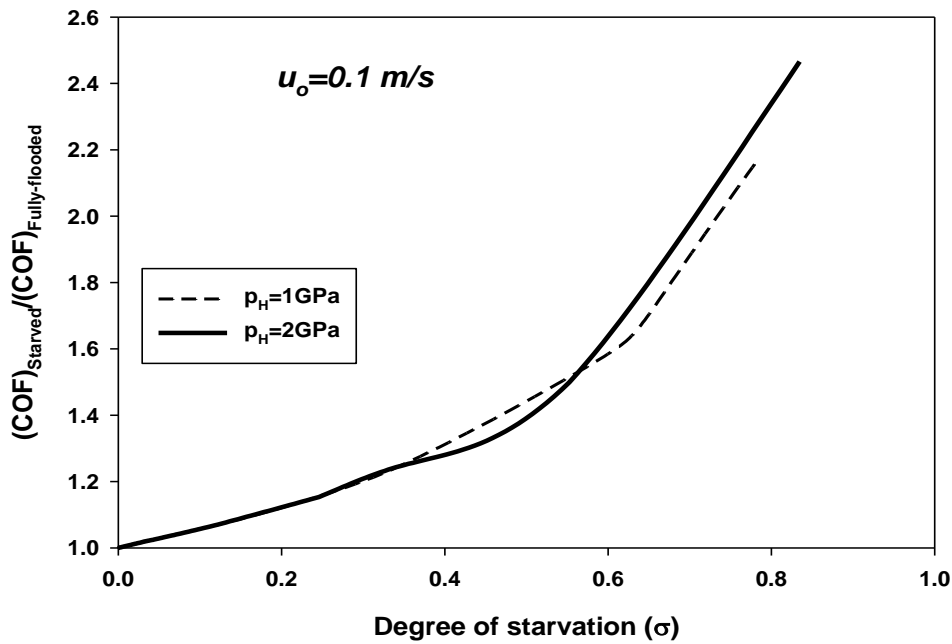
Fig. 4 : Variation of the factor by which the coefficient of friction increases with the degree of starvation for different Hertzian pressures at u_o=0.1 m/s, α=20 GPa^{-1} and R=0.02 m
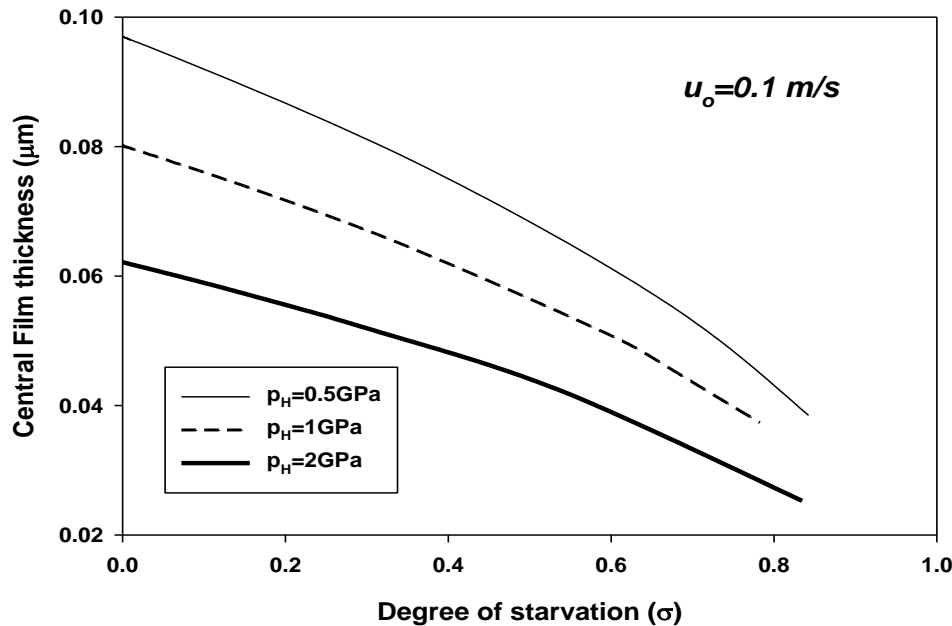

Fig. 5 : Variation of central film thickness with the degree of starvation for different Hertzian pressures at u_o=0.1 m/s, α=20 GPa^{-1} and R=0.02 m

4.2 Effect of Rolling Speed

Since rolling speed is an important parameter affecting starvation, Fig. 6 compares the variation of the degree of starvation (σ) with the position of inlet meniscus (X_{in}) for three rolling speeds (u_o=0.1, 1 and 10 m/s) while the maximum Hertz pressure is kept constant at p_H=1GPa. It can be seen from Fig. 6 that the general trend of variation of σ is the same as described earlier with reference to Fig. 1, i.e., a gradual increase followed by a steep rise as the inlet meniscus is shifted towards the contact zone. Further, it is apparent that the degree of starvation for a particular position of inlet meniscus is larger at higher rolling speed. This observation is consistent with the practical experience which indicates more likelihood of starvation at higher speeds. This is due to the fact that a larger amount of lubricant is dragged within the conjunction at higher speeds resulting in thicker films, therefore, in the case of inadequate lubricant supply, high speed contacts are starved to a greater extent. Furthermore, at higher speeds, the fluid pressure starts building up farther away from the contact zone and hence, fully flooded condition is ensured by selecting a sufficiently large negative value of X_{in} while carrying out EHL simulations at high rolling speeds.

In order to further investigate the influence of speed on starvation effects, Figs. 7 and 8, pertaining to u_o=1 and 10m/s respectively, compare the pressure distributions and film profiles obtained for X_{in} = -6 and -1.05 at p_H=1GPa. It can be seen that the contact zone pressures for the case of lower speed (Fig. 7) remain unaffected by starvation, whereas, at higher speed (Fig. 8), the contact zone pressures under starved condition (X_{in}=-1.05) are slightly higher than the corresponding pressures under fully flooded condition (X_{in}=-6). Also, the film-thinning attributed to starvation is more pronounced at higher rolling speed. This is obviously due to the fact that the inlet pressure at higher speed sweeps a longer distance and attains a higher value at the entry to the contact zone. Hence, in order to balance the applied load, the contact zone pressures rise slightly above the corresponding fully flooded values.

Fig. 9 compares the starvation effect on coefficient of friction by showing the variation of (COF)$_{Starved}$/(COF)$_{Fully-flooded}$ with the degree of starvation at three rolling speeds (u_o=0.1, 1 and 10 m/s) for p_H=1GPa. It can be seen that coefficient of friction increases gradually by factors much below 10 for degrees of starvation less than 0.97; however, as σ approaches close to 1, the coefficient of friction increases steeply by factors exceeding 30! Such high factors are obtained at u_o=10 m/s where the degree of starvation achieved is maximum for the range of X_{in} considered here. It is quite interesting to see that the curves pertaining to the three rolling speeds collapse into a single curve, which suggests that (COF)$_{Starved}$/(COF)$_{Fully-flooded}$ is independent of rolling speed for a particular degree of starvation.

Fig. 10 shows the variation of central film thickness with degree of starvation for the same operating conditions as in Fig. 9. It can be seen that as the degree of starvation increases, the central film thickness decreases with a slope which increases with increasing rolling speed. At u_o=10 m/s, the fully-flooded film thickness is much higher and hence, the slope of the corresponding curve undergoes an abrupt increase as the degree of starvation approaches 1. As observed earlier in Fig. 5, the central film thickness at the three rolling speeds converge to a single value under highly starved condition.
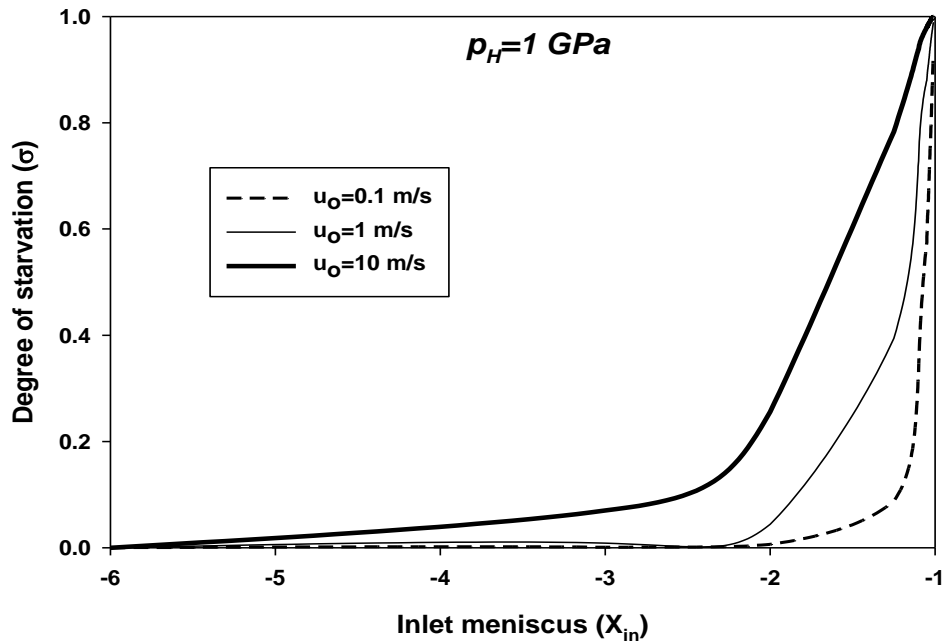
Fig. 6 : Variation of the degree of starvation with the position of the inlet meniscus for different rolling speeds at p_H=1 GPa, α=20 GPa^{-1} and R=0.02 m
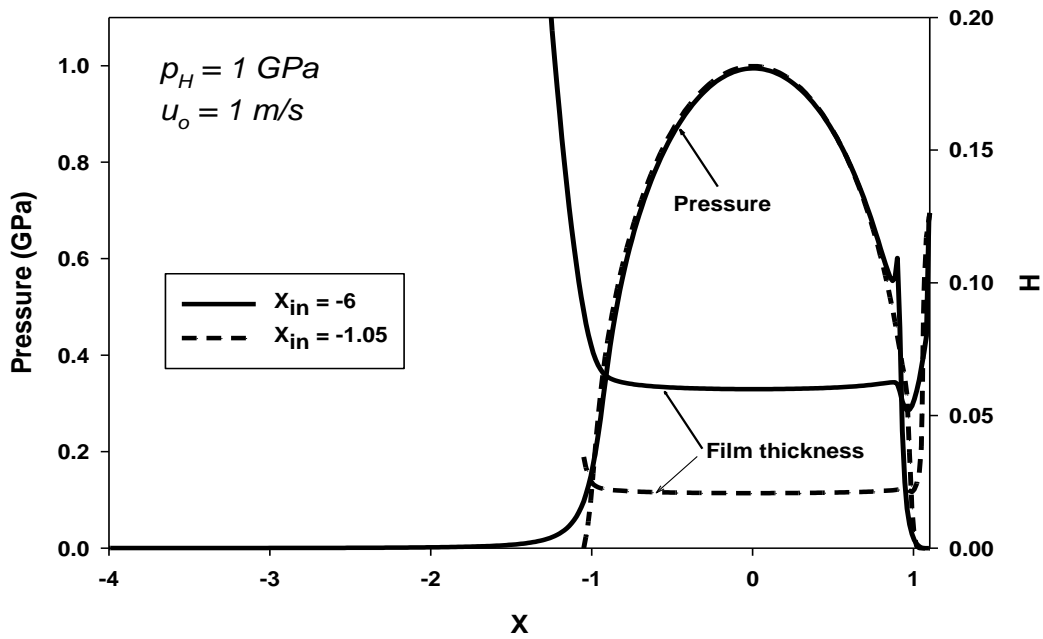

Fig. 7: Comparison of pressure distributions and film shapes at two different positions of inlet meniscus for p_H=1 GPa, u_o=0.1 m/s, α=20 GPa^{-1} and R=0.02 m
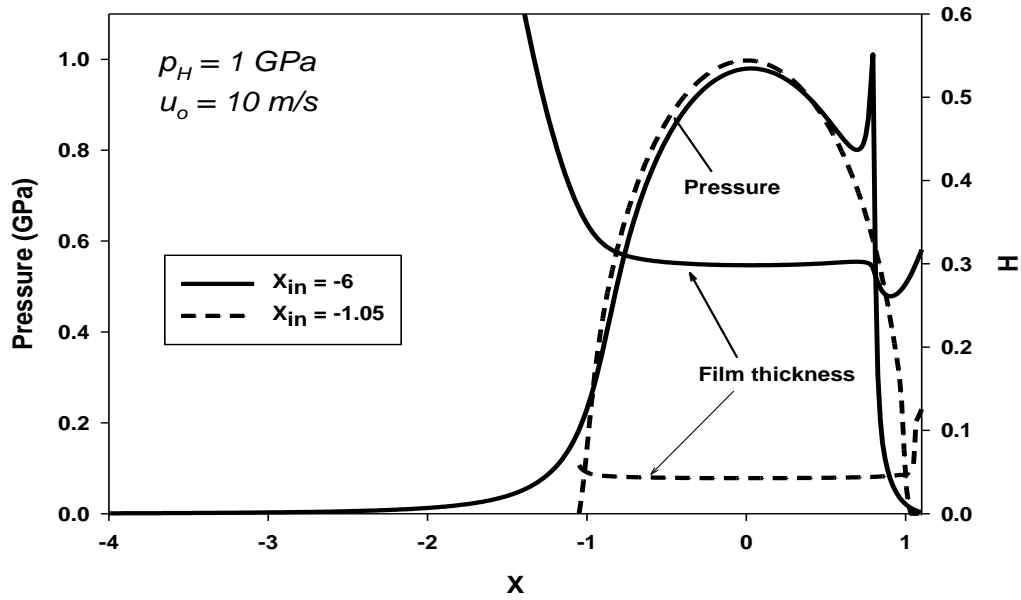
Fig. 8 : Comparison of pressure distributions and film shapes at two different positions of inlet meniscus for p_H=1 GPa, u_o=10 m/s, α=20 GPa^{-1} and R=0.02 m
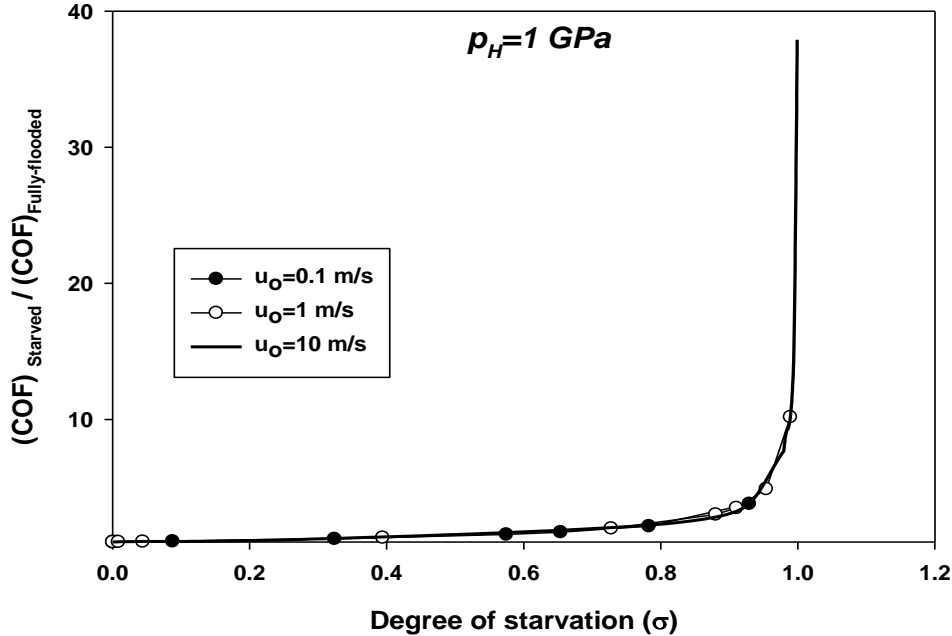

Fig. 9 : Variation of the factor by which the coefficient of friction increases with the degree of starvation for different rolling speeds at p_H=1 GPa, α=20 GPa^{-1} and R=0.02 m
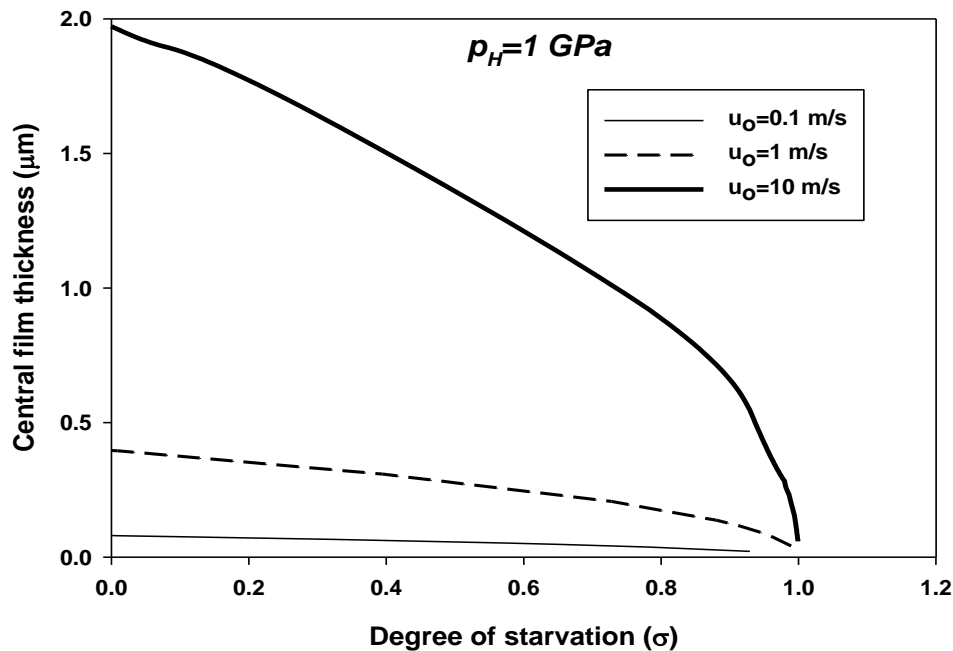
Fig. 10: Variation of central film thickness with the degree of starvation for different rolling speeds at p_H=1 GPa, α=20 GPa^{-1} and R=0.02 m

5. Conclusions

The starvation effect is modeled by shifting the position of the inlet meniscus towards the contact zone. The degree of starvation, so obtained, is plotted as a function of the position of inlet meniscus under different operating conditions. The effect of starvation on coefficient of friction and central film thickness has been studied at different loads and rolling speeds. Some of the salient conclusions are outlined below:

1) Film-thinning is the most serious consequence of inadequate filing of the EHL conjunction as it may lead to film failure leading to metal-metal contact and hence, increased friction and wear.
2) Starvation causes an increase in the value of coefficient of friction (COF). This effect has been quantified in terms of the ratio of COF values obtained under starved and fully flooded conditions.
3) At higher load, the maximum increase in COF is higher. The reason for this increase in COF is the increased shear rates due to the film-thinning attributed to starvation. This increase in the shear rate results in higher shear stresses and hence, higher coefficient of friction.
4) Degree of starvation and the central film thickness tends to converge to a common value independent of the load.

5) Rolling speed is an important parameter affecting starvation. The degree of starvation for a particular position of inlet meniscus is found to be larger at higher rolling speed. This is in consonance with the practical experience of more frequent occurrence of starvation at higher speeds. This is due to the fact that larger amount of lubricant is required to produce thicker fluid films associated with high speed EHL contacts.

6) The film-thinning attributed to starvation is more   pronounced at higher rolling speed as the inlet pressure sweeps a longer distance and attains a higher value at the entry to the contact zone.

7) As the degree of starvation increases, the central film thickness decreases with a slope which increases with increasing rolling speed.

References

[1]   Hsiao, H.S. and Hamrock, B. J. Non-Newtonian and thermal effects on film generation and traction reduction EHL line contact conjunction. ASME, J.Tribol. 1994, 116, 559-568.

[2]   Salehizadeh, H. and Saka, N. Thermal non-Newtonian elastohydrodynamic lubrication of rolling line contacts. ASME, J. Tribol., 1991, 113, 181-191.

[3]   Sui, P. C and Sadeghi, F. Non-Newtonian thermal elastohydrodynamic lubrication. ASME, J. Tribolo., 1991,113, 390-397.

[4]   Wang, J. M. and Aronov, V. Thermal elastohydrodynamic lubrication of non-Newtonian fluids with rough surfaces. ASME, J. Tribol., 1997, 119, 605-612.

[5]   Wolf, R. and Kubo, A. A generalized non- Newtonian fluid model introduction into elasohydrodynamic lubrication. ASME, J. Tribol., 1996,118, 74-82.

[6]   Lee, R. T., and Hamrock, B. J., 1990, "A Circular Non- Newtonian Fluid Model: Part 1-Used in Elastohydrodynamic Lubrication," ASME J. Tribol., 112,pp. 486-496.

[7]   Khonsari, M., and Hua, D., 1994 "Thermal Elastohydrodynamic Analysis Using a Generalized Non-Newtonian With Application to Bair-Winer Constitutive Equation," ASME J. Tribol., pp. 37-46.

[8]   Damiens, B., Venner, C. H., Cann, P. M. E., and Lubrecht, A. A., 2004, "Starved Lubrication of Elliptical EHD Contacts, " ASME J.Tribol., 126, pp. 105-111.

[9]   Chevalier, F., Lubrecht, A. A., Cann, P. M. E., Colin, F., and Dalmaz, G., 1998, "Film Thickness in Starved EHL Point Contacts," ASME J. Tribol., 120, pp. 126-133